PASJ: Publ. Astron. Soc. Japan **56**, L5–L8, 2004 April 25

X-Ray Expanding Features Associated with a Moreton Wave

Noriyuki NARUKAGE, Taro MORIMOTO, Miwako KADOTA, Reizaburo KITAI,
Hiroki KUROKAWA, and Kazunari SHIBATA
Kwasan and Hida Observatories, Kyoto University, Yamashina, Kyoto 607-8471
naru@kwasan.kyoto-u.ac.jp

(Received 2003 November 22; accepted 2004 February 3)

Abstract

We report on the simultaneous observation of a Moreton wave in Hα and two kinds of coronal expanding features in soft X-rays near the solar limb. We consider the faster X-ray feature and the slower one as being an "X-ray wave" and "ejecta", respectively. The chromospheric Moreton wave propagated on the solar disk at a speed of $1040 \pm 100\,\mathrm{km\,s^{-1}}$, whereas the coronal X-ray wave propagated outside of the disk toward the outer corona at $1400 \pm 250\,\mathrm{km\,s^{-1}}$. We identified the X-ray wave as MHD fast-mode shock. The fast-mode Mach number (M_f) of the X-ray wave was also estimated to be about 1.13–1.31, which decreases during propagation. The timing when the M_f became "1" is consistent with that of the disappearance of the Moreton wave. Moreover, we discuss the 3-dimensional structure of the shock wave and the relation between the shock wave and the ejecta (and Hα filament eruptions).

Key words: shock waves — Sun: chromosphere — Sun: corona — Sun: flares

1. Introduction

Moreton waves are flare-associated waves observed to propagate across the solar disk in Hα (Moreton 1960; Smith, Harvey 1971). They propagate at speeds of 500–1500 $\mathrm{km\,s^{-1}}$ with arc-like fronts in somewhat restricted angles, and are often associated with type-II radio bursts (Kai 1969). The Moreton wave has been identified as the intersection of a coronal MHD fast-mode weak shock wave and the chromosphere (Uchida 1968, 1974). However, the generation mechanism of a Moreton wave has not yet been cleared.

Recently, many large-scale coronal transients have been discovered using the Extreme ultraviolet Imaging Telescope (EIT) on board Solar and Heliospheric Observatory (SOHO). These features are now commonly called "EIT waves" (Thompson et al. 1998; Klassen et al. 2000; Eto et al. 2002).

Moreover, the Soft X-ray Telescope (SXT) on board Yohkoh discovered wave-like disturbances in the solar corona associated with flares (Khan, Hudson 2000; Hudson et al. 2003), which we call "X-ray waves" in this paper. Two simultaneous observations of Moreton waves and X-ray waves were reported (Khan, Aurass 2002; Narukage et al. 2002). In this paper, we report on a third example, which was observed near the solar limb on 2000 March 3.

The purpose of this paper is to consider the properties of a flare-associated MHD shock wave based on the simultaneous observation of a Moreton wave and two kinds of X-ray expanding features observed near the solar limb. We consider the faster X-ray feature and the slower one as being an "X-ray wave" and "ejecta", respectively. Therefore, we examine the X-ray wave and identify it as an MHD fast-mode shock. The fast-mode Mach number (M_f) of the shock wave decreased during the propagation. We found a relationship between M_f and the disappearance of the Moreton wave. Moreover, in this event the 3-dimensional structure of the shock wave was clearly revealed by the Moreton wave and the X-ray wave. The relation between the shock wave and the ejecta (and Hα filament eruptions) is also discussed.

In section 2, the instrumentation and observing methods are summarized. In section 3, the results of analyses of the Moreton wave and the X-ray wave are described. In section 4, a summary and a discussion are given.

2. Observations

We observed a Moreton wave and X-ray features associated with an M-class flare in NOAA Active Region 8882 at S15, W60 on 2000 March 3. The flare started at 02:08 UT and peaked at 02:14 (GOES times).

The Moreton wave was observed in Hα (line center and $+/-$ 0.8 Å) with the Flare Monitoring Telescope (FMT) (Kurokawa et al. 1995) at Hida Observatory of Kyoto University. The FMT observed four full-disk images (in the Hα line center and $+/-$ 0.8 Å, and continuum) and one solar limb image (in the Hα line center). These images were observed co-temporal. The time resolution of the images used in the present work was 14 s, though the FMT operated at a higher time resolution. The pixel size was $4''\!.2$.

The X-ray wave and ejecta were observed in soft X-rays with Yohkoh/SXT (Tsuneta et al. 1991). The SXT is sensitive to soft X-ray photons in the energy range $\sim$ 0.28–4 keV, which corresponds to wavelengths $\sim$ 3–45 Å. We used partial frame images observed with an Al-Mg filter. The observing time cadence was 14 s. The pixel sizes of the half and quarter-resolution images were $4''\!.91$ and $9''\!.82$, respectively.

The magnetic field of the photosphere was observed with the Michelson Doppler Imager (MDI) (Scherrer et al. 1995) on board SOHO. The time resolution and pixel sizes are about 90 min and $2''$, respectively. A metric type-II radio burst was recorded with the Hiraiso Radio Spectrograph (HiRAS)

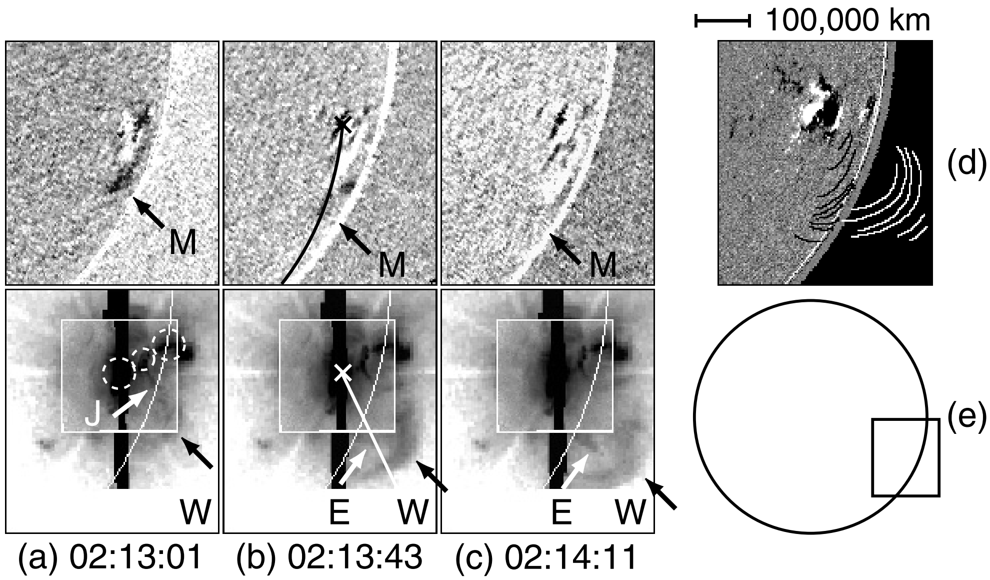

Fig. 1. Observed images on 2000 March 3, at NOAA AR 8882. Top panels of images (a)–(c) are Hα $+0.8\,$Å "running difference" images of a Moreton wave (black arrows "M"). Bottom panels of images (a)–(c) are negative soft X-ray images of an X-ray wave (black arrows "W"), ejecta (white arrows "E") and a jet (white arrow "J") taken with the Al-Mg filter. The images inside and outside the boxes are half-resolution ($4''.91$) and quarter-resolution ($9''.82$) images, respectively. The white dashed circles in image (a) show the bright regions in soft X-rays. The crosses and lines in image (b) are the flare site and measures of the wave, respectively. We assume that the brightest region in Hα is the flare site. Image (d) shows the wave fronts of the Moreton wave from 02:12:01 to 02:15:01 UT (black lines) and the X-ray wave from 02:13:01 to 02:14:11 UT (white lines) overlaid on the photospheric magnetic field observed at 01:35:02 UT. These wave fronts were determined visually. The box and circle shown in image (e) are the field of view of images (a)–(d) and the limb of the Sun, respectively.

(Kondo et al. 1995).

3. Results

Figure 1 shows the observed images on 2000 March 3 of NOAA AR 8882. The top panels of images (a)–(c) are "running difference" images (where each image has the image before one minute subtracted from it) observed in Hα $+0.8\,$Å. The running-difference method clearly shows the motion of the Moreton wave. The bottom panels are the negative soft X-ray images. There are two kinds of expanding features shown by the black arrows, "W", and the white arrows, "E". In the flare, the three regions indicated by the white dashed circles in image (a) brightened in soft X-rays. When the flare occurred, the left and right regions became bright at the same time and feature "W" expanded from the left region. After several tens of seconds, we observed the brightening and a jet-like feature, "J", at the center region.

There are two possibilities: either feature "W" is an "erupting loop" or an "X-ray wave". If "W" is an "erupting loop", the edges (i.e., footpoints) should be fixed on the solar disk. However, the southern edge of "W" moved southward and was located just above the propagating Moreton wave (see figures 1 and 3). Meanwhile, the apparent northern footpoint, shown by the white arrow, "J", seems to be fixed. However, because of the time lag between the X-ray brightenings related to "W" and "J", we think "W" and "J" are not parts of the same loop. Hence we consider "W" is not an "erupting loop" but instead an "X-ray wave". "E" and "J" are considered to be "ejecta" and a "jet", respectively.

In image (d), the apparent positions of the wave fronts are overlaid on the longitudinal magnetogram from MDI. The Moreton wave (black lines) can be identified visually from 02:12:01 to 02:15:01 UT, and the X-ray wave (white lines) from 02:13:01 to 02:14:11 UT. The chromospheric Moreton wave propagated on the solar disk, whereas the coronal X-ray wave propagated toward the outer corona. The field of view is illustrated by the box in figure 1 (e).

Figures 2 (f) and (g) show timeslice images of the Moreton wave along the great circle and the X-ray expanding features along the plane-of-sky, respectively. The propagation speeds of the Moreton wave and the X-ray wave derived from the timeslice images are roughly constant at $1040 \pm 100\,\mathrm{km\,s^{-1}}$ and $1400 \pm 250\,\mathrm{km\,s^{-1}}$, respectively. In fact, the Moreton wave seems to be somewhat decelerating. The ejecta, "E", moved at speeds of $490\,\mathrm{km\,s^{-1}}$.

4. Discussion

In Uchida's model (1968, 1974), a Moreton wave is a sweeping skirt on the chromosphere of a weak MHD fast-mode shock that propagates in the corona. This model thus also explains the meter-wave type-II radio burst as a signature of the coronal propagation, and predicts the existence of a coronal counterpart of the chromospheric Moreton wave. There is the possibility that the X-ray wave is a coronal counterpart of the Moreton wave. One case of the X-ray wave was examined using MHD theory, and was identified as an MHD fast-mode shock (Narukage et al. 2002).

In this event, the flare occurred near the solar limb. Hence the chromospheric Moreton wave propagated on the solar disk, whereas the coronal X-ray wave propagated toward the outer

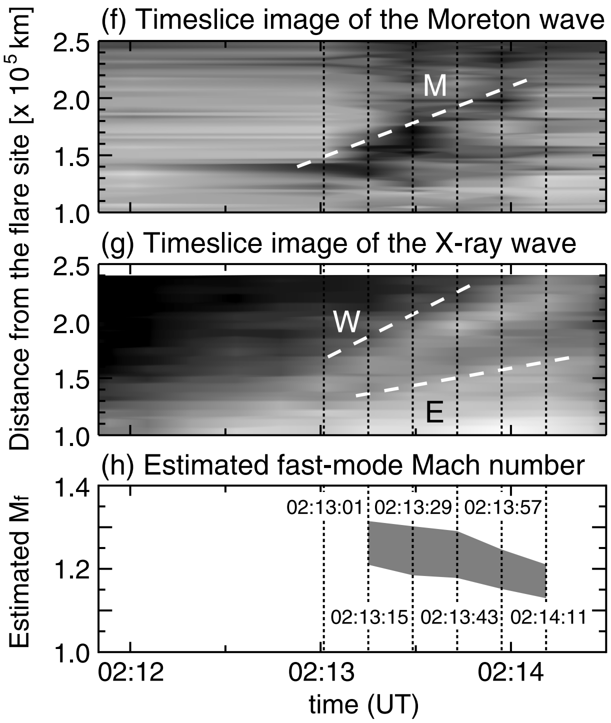

Fig. 2. Timeslice images and estimated fast-mode Mach number. Image (f) is the timeslice image of the Hα images along the great circle [black line in figure 1 (b)]. Image (g) shows the timeslice image of the soft X-ray images along the plane-of-sky [white line in figure 1 (b)]. The speeds of the Moreton wave, "M", the X-ray wave, "W", and the ejecta, "E", derived from the timeslice images are $1040\,\mathrm{km\,s^{-1}}$, $1400\,\mathrm{km\,s^{-1}}$, and $490\,\mathrm{km\,s^{-1}}$, respectively. The gray area of image (h) is the range of the estimated fast-mode Mach number.

corona. The direction of propagation of the X-ray waves disagrees with those of the Moreton wave [figure 1 (d)]. However, the propagation speeds are comparable. Considering the 3-dimensional structure, we can say that these results are not inconsistent with the assumption that the X-ray wave is the coronal counterpart of the Moreton wave.

4.1. *Examination Whether the X-Ray Wave is an MHD Fast-Mode Shock*

The Hiraiso Radio Spectrograph (HiRAS) recorded a metric type-II radio burst when the X-ray wave was observed. The type-II radio burst indicates the existence of an MHD shock wave. Based on Mann's coronal electron density model (Mann et al. 1999), we can calculate the source height from the photosphere as being 223000 km at 02:14 and 417000 km at 02:16, and hence the speed of the shock wave as being $1600 \pm 300\,\mathrm{km\,s^{-1}}$. The source height at 02:14 is consistent with the X-ray features [see figure 2 (g)]. Mancuso et al. (2002) also reported the speed of the same shock wave as being $1100\,\mathrm{km\,s^{-1}}$ using another density model. These are roughly consistent with the propagation speed of the X-ray wave, $1400 \pm 250\,\mathrm{km\,s^{-1}}$. Hence, there is the possibility that the X-ray wave is a coronal MHD shock wave.

Assuming that the X-ray wave is fast shock, we can estimate its propagation speed, based on MHD shock theory (Rankine–Hugoniot relation) and the observed soft X-ray intensities (I_X) ahead of (i.e., in region 1) and behind (i.e., in region 2) the X-ray wave front. If this estimated speed of the shock is consistent with the observed propagation speed of the X-ray wave, we can conclude that the X-ray wave is a fast shock.

If we know (I_{X1}, T_1, B_1, θ_1, I_{X2}), we can find (v_1, T_2, B_2, θ_2, v_2) (see Narukage et al. 2002). We measure I_{X1} and I_{X2} observed at 02:13:15, 02:13:29, 02:13:43, 02:13:57, and 02:14:11 UT, and obtain I_{X2}/I_{X1} = 3.74, 4.18, 4.02, 3.35, and 2.83, respectively. The temperature (T_1) was calculated using pre-flare full frame images taken with the thin Al and Al-Mg filters of SXT (Tsuneta et al. 1991) as T_1 = 2.25–2.75 MK at 02:13:15 UT and T_1 = 2.00–2.50 MK at 02:13:29–02:14:11 UT. Substituting this T_1 into the SXT response function gave the emission measure. We calculated the coronal density (ρ_1) as $10^{8.3}$–$10^{8.6}\,\mathrm{cm^{-3}}$, assuming that the line-of-sight thickness (l) of the observed region was the coronal pressure scale-height (1.00–1.38×10^5 km for 2.00–2.75 MK). The l is comparable to the scale of the waves, and the estimated ρ_1 is consistent with the real coronal density. The photospheric magnetic field strength (B_{p1}) was observed by MDI, and we assumed that the coronal magnetic field strength (B_1) was 1/3 or 1/2 of B_{p1} (Dere 1996). When $\theta_1 = 90°$, the shock is perpendicular, and $\theta_1 = 60°$ corresponds to an oblique shock. These observational properties give the propagation speed of the shock ($v_{sh} = v_1 \cos\theta_1$). The estimated fast shock speed, 900–1900 $\mathrm{km\,s^{-1}}$, is in rough agreement with the observed propagation speed of the X-ray wave, $1400 \pm 250\,\mathrm{km\,s^{-1}}$.

The above examinations suggest that the X-ray wave is a fast shock propagating through the corona. The fast-mode Mach number of the X-ray wave was also estimated to be 1.13–1.31 using the estimated shock speeds. These values indicate that the propagation speed of the Moreton wave is comparable to the MHD fast-mode speed, and consistent with Uchida's model of a weak MHD fast-mode shock. Deceleration of the Moreton wave can be seen in figure 2 (f). This is in accordance with the results of Warmuth et al. (2001). We can see that the X-ray wave (fast shock) becomes wider, i.e., diffuses, in figure 2 (g), and that the estimated fast-mode Mach number decreases in figure 2 (h). The decrease rate is $-0.0016\,\mathrm{s^{-1}}$. After 02:14:11 UT, the X-ray wave propagated outside of the field of view. If the Mach number decreased at the same rate, at 02:16:10 UT the Mach number would become "1". The timing roughly agrees with the timing of the disappearance of the Moreton wave. In the Uchida model, the front of the Moreton wave is identified as the region of downward motion in the chromosphere caused by the coronal shock wave. Our result is clear evidence for the Uchida model.

4.2. *3-D Structure of the Flare-Associated Shock Wave*

The flare occurred near to the solar limb. Hence, the chromospheric Moreton wave propagated on the solar disk, whereas the coronal X-ray wave propagated toward the outer corona (figure 1). These two kinds of waves seem to be different. However, the above result suggests that these two waves are the same flare-associated waves.

Figure 3 shows the Moreton wave (left panels) and the X-ray wave (center panels) at 02:13:01 and 02:13:43 UT. The spheres in figures 3 (i) and (j) are centered on the flare site and have radii of 150000 km and 200000 km, respectively. In the

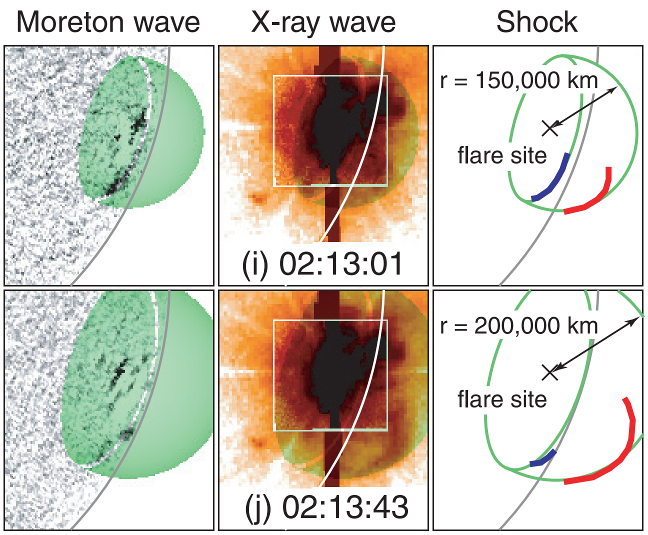

Fig. 3. Observation of the 3-dimensional structure of the flare-associated shock wave. The left and center panels show Hα +0.8 Å "running difference" images of the Moreton wave and negative soft X-ray images of the X-ray wave, respectively. Images (i) and (j) were observed at 02:13:01 and 02:13:43 UT. The center of the spheres is located at the flare site and the radii in images (i) and (j) are 150000 km and 200000 km, respectively. The right panels show outline images of the shock wave. The lines are the wavefronts of the Moreton wave (blue lines) and the X-ray wave (red lines).

outline images (right panels), the wavefront of the Moreton waves (blue lines) corresponds to the intersection of the sphere and the solar disk, whereas the X-ray waves (red lines) seem to be along the sphere. Hence, in the simplest approximation (symmetrical shock expansion), the propagation of these two waves indicates the 3-dimensional structure of the flare-associated shock wave (spheres).

4.3. *Relation between the X-Ray Wave and the Ejecta*

In this event, the ejecta, "E", were observed behind the X-ray wave, "W", and moved at a speed of 490 km s^{-1}. In the early phase of the shock observation (at 02:13:15 UT), $X \equiv \rho_2/\rho_1 = v_1/v_2$ is 1.3–1.4. If a one-dimensional approximation is assumed around the shock front, $v_{sh}/v_{ejecta} = v_1/(v_1 - v_2) = X/(X-1)$ and v_{ejecta} is estimated to be 330–400 km s^{-1}, where v_{ejecta} is the speed of the ejecta. This value is roughly consistent with the observed speed of the ejecta, "E". In figure 2 (g), the dashed line "E" intersects the dashed line "W" at about 02:12:20 UT. At this time, the Moreton wave was already observed. Based on these results, we suggest that the shock may not have been driven by the ejecta, but instead the ejecta may have been accelerated by the shock. However, we cannot really distinguish this possibility from the other scenario, where the ejecta is launched either by the same process that launches the wave, or by another closely related mechanism (e.g., loss of magnetic equilibrium).

Finally, we discuss the relation between Moreton waves and filament eruptions. In all of the Moreton wave events observed at Hida observatory, Hα filaments erupted in the same direction after the waves propagated (e.g., Eto et al. 2002). Before the eruption, the filaments were invisible in Hα. In this event, the filament eruption became visible at 02:22 UT in Hα −0.8 Å. We consider these filament eruptions to be closely related to the Moreton waves as well as the ejecta, "E".

The authors thank all members of the Kwasan and Hida Observatories for useful comments. The Yohkoh satellite is a Japanese national project, launched and operated by ISAS, and involving many domestic institutions, with multilateral international collaboration with the US and the UK. SOHO is a mission of international cooperation between European Space Agency (ESA) and NASA. The Hiraiso Radio Spectrograph (HiRAS) is operated by Hiraiso Solar Terrestrial Research Center, and monitoring solar radio bursts.

We are deeply grateful to the late Dr. Yutaka Uchida and pray for the repose of his soul. We dedicate this paper to his memory.

References

Dere, K. P. 1996, ApJ, 472, 864
Eto, S., et al. 2002, PASJ, 54, 481
Hudson, H. S., Khan, J. I., Lemen, J. R., Nitta, N. V., & Uchida, Y. 2003, Sol. Phys., 212, 121
Kai, K. 1969, Sol. Phys., 10, 460
Khan, J. I., & Aurass, H. 2002, A&A, 383, 1018
Khan, J. I., & Hudson, H. S. 2000, Geophys. Res. Lett., 27, 1083
Klassen, A., Aurass, H., Mann, G., & Thompson, B. J. 2000, A&AS, 141, 357
Kondo, T., Isobe, T., Igi, S., Watari, S., & Tokumaru, M. 1995, J. Commun. Res. Lab., 42,111
Kurokawa, H., Ishiura, K., Kimura, G., Nakai, Y., Kitai, R., Funakoshi, Y., & Shinkawa, T. 1995, J. Geomag. Geoelectr., 47, 1043
Mancuso, S., Raymond, J. C., Kohl, J., Ko, Y.-K., Uzzo, M., & Wu, R. 2002, A&A, 383, 267
Mann, G., Jansen, F., MacDowall, R. J., Kaiser, M. L., & Stone, R. G. 1999, A&A, 348, 614
Moreton, G. E. 1960, AJ, 65, 494
Narukage, N., Hudson, H. S., Morimoto, T., Akiyama, S., Kitani, R., Kurokawa, H., & Shibata, K. 2002, ApJ, 572, L109
Scherrer, P. H., et al. 1995, Sol. Phys., 162, 129
Smith, S. F., & Harvey, K. L. 1971, in Physics of the Solar Corona, ed. C. J. Macris (Dordrecht: Reidel), 156
Thompson, B. J., Plunkett, S. P., Gurman, J. B., Newmark, J. S., St. Cyr, O. C., Michels, D. J., & Delaboudinière, J.-P. 1998, Geophys. Res. Lett., 25, 2465
Tsuneta, S., et al. 1991, Sol. Phys., 136, 37
Uchida, Y. 1968, Sol. Phys., 4, 30
Uchida, Y. 1974, Sol. Phys., 39, 431
Warmuth, A., Vršnak, B., Aurass, H., & Hanslmeier, A. 2001, ApJ, 560, L105